

Residual arsenic site in oxidized $\text{Al}_x\text{Ga}_{1-x}\text{As}$ ($x=0.96$)

S.-K. Cheong,^{a)} B. A. Bunker, and T. Shibata

Department of Physics, University of Notre Dame, Notre Dame, Indiana 46556

D. C. Hall, C. B. DeMelo, Y. Luo, and G. L. Snider

Department of Electrical Engineering, University of Notre Dame, Notre Dame, Indiana 46556-5637

G. Kramer and N. El-Zein

Motorola Inc., Physical Sciences Research Laboratory, Tempe, Arizona 85284

(Received 11 September 2000; accepted for publication 23 February 2001)

X-ray absorption fine-structure spectroscopy is used to determine the site of residual As in wet-oxidized $\text{Al}_{0.96}\text{Ga}_{0.04}\text{As}$. In a $\sim 0.5\text{-}\mu\text{m}$ -oxide film removed from its GaAs substrate, the remaining As atoms are found to be coordinated with oxygen in the form of amorphous-As oxides, with a mixture of $\sim 80\%$ As^{3+} and $\sim 20\%$ As^{5+} sites that are locally similar to As_2O_3 and As_2O_5 . No evidence of interstitial or substitutional As, As precipitates, or GaAs is seen, implying that less than 10% of the As atoms are in these forms. © 2001 American Institute of Physics.

[DOI: 10.1063/1.1367307]

Wet-thermal native oxides of AlGaAs (Ref. 1) have led to numerous advances in optoelectronic devices² and have been explored for their potential use in GaAs-based metal-oxide-semiconductor electronic applications.³ While most of the As in the semiconductor crystal leaves during oxidation, residual quantities have been correlated to bulk oxide leakage current, and to interfacial traps that increase interface recombination and produce Fermi-level pinning.⁴ Hydrogen liberated in the wet-oxidation reaction is believed to play an important role in reducing As_2O_3 to As, and possibly As to AsH_3 , volatile species which can more readily escape the oxide film.⁵ Yet the degree to which, and the form in which, As remains are still not well understood. Crystalline As, amorphous As, and amorphous As_2O_3 have been observed via Raman spectroscopy⁴⁻⁶ in partially oxidized AlGaAs films, with As scattering dropping to barely detectable levels after full oxidation. In higher leakage films, it has been suggested that As precipitates may occupy up to $\sim 6\%$ of the oxide volume.⁴ However, chemical analysis of other AlGaAs oxides have shown residual As levels of <2 at. %, with no evidence of As precipitates.⁷

In this letter, we present the results of x-ray absorption fine-structure spectroscopy (XAFS) studies on the form and site of residual As within the bulk of AlGaAs native-oxide films. The XAFS technique⁸ is sensitive to the local structure about a chosen atomic species, revealing the types of nearby atoms and the radial distance distributions to these neighbors. By carefully measuring the XAFS spectra near the absorption threshold, x-ray absorption near-edge structure (XANES) can also often be used to determine formal charge-state and site symmetry.⁹

The sample used for this study is grown by molecular-beam epitaxy on semi-insulating GaAs and consists of a 7000 Å GaAs buffer layer, 5000 Å $\text{Al}_x\text{Ga}_{1-x}\text{As}$ ($x\sim 0.96$), and a 200 Å GaAs cap layer. All layers are not intentionally doped. After selectively removing the GaAs cap layer in a

4:1 citric acid: H_2O_2 etch, a 1 cm \times 4 cm sample is loaded into a 2-in.-diam quartz tube furnace (400 °C). After heating for 2 min under a dry N_2 purge, oxidation of the AlGaAs layer proceeds as water vapor is introduced for 8 min via bubbling 0.66 l/min N_2 through 95 °C H_2O . To study the As specifically in the oxide film in isolation of the GaAs substrate, the sample is subsequently mounted oxide down on a glass slide using low-temperature wax and the substrate is chemically removed. A phosphoric-acid-hydrogen-peroxide etch (4:1:50 H_3PO_4 : H_2O_2 : H_2O) is used to thin the substrate, the remainder of which is then removed by the slower, oxide-selective 4:1 citric peroxide etch.

For calibration standards used in the XAFS analysis, elemental As (As^0), GaAs, As_2O_3 (As^{3+}), and As_2O_5 (As^{5+}) are obtained from standard chemical supply houses. The standard samples are ground with mortar and pestle and sieved to 400 mesh ($<40\ \mu\text{m}$) inside an inert-atmosphere glovebox. These compounds are all characterized using x-ray diffraction (XRD) to verify their phase purity. We have observed in these measurements that the elemental As and As_2O_5 powder are unstable in contact with air; to alleviate this problem, these samples are kept in air-tight cells and surrounded with dry nitrogen during all measurements. Subsequent XRD analysis shows negligible degradation.

XAFS measurements about the As *K* edge are performed at the Advanced Photon Source (APS) using the Materials Research Collaborative Access Team (MRCAT) undulator beamline¹⁰ over the energy range 11 667–12 900 eV. XAFS data are measured in fluorescence mode on the oxidized $\text{Al}_{0.96}\text{Ga}_{0.04}\text{As}$ film, but in transmission mode on As-rich standard samples where fluorescence spectra are susceptible to distortion.

XANES spectra for this work are used to “fingerprint” the As site. The main feature of As *K*-edge XANES spectra is the abrupt increase in absorption that occurs over a 10 eV range beginning at $\approx 11\ 863$ eV for As^0 and at $\approx 11\ 870$ eV for As^{5+} compounds. This absorption edge (E_0) shifts higher with increasing As oxidation state. For analysis of XANES, the x-ray energy origin is set at 11 867 eV (*K* edge of As^0).

^{a)}Electronic mail: scheong@nd.edu

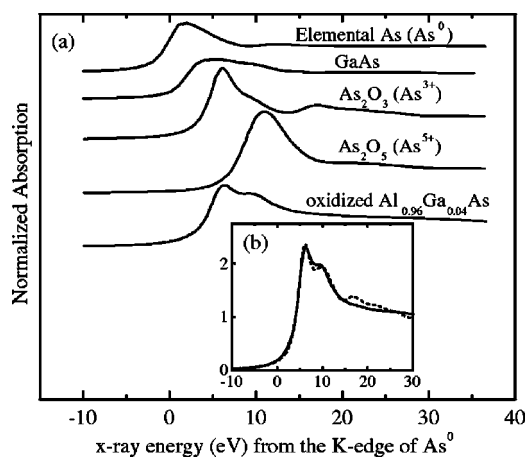


FIG. 1. (a) XANES spectra of the oxide film (oxidized $\text{Al}_{0.96}\text{Ga}_{0.04}\text{As}$) and powders of elemental As, GaAs, As_2O_3 , and As_2O_5 ; (b) oxide film spectra (solid line) compared with a sum of 80% As_2O_3 and 20% As_2O_5 (dotted line).

The pre-edge background is subtracted by fitting a linear polynomial function through the region -200 to -30 eV and normalized by dividing by the edge step. The As K -edge XANES spectra of standard compounds (As^0 , GaAs, As^{3+} , and As^{5+}) and the oxidized $\text{Al}_{0.96}\text{Ga}_{0.04}\text{As}$ sample are shown in Fig. 1(a). None of these compounds singly matches well with the AlGaAs native oxide. The XANES spectrum of the oxide film shows that the sample contains primarily As^{3+} , with the additional feature at 10 eV indicating the presence of As^{5+} species. The best fit to the spectrum (-10 – 30 eV), shown in Fig. 1(b), is obtained from a combination of 80% As_2O_3 and 20% As_2O_5 ; uncertainties are estimated as $\pm 10\%$ of these values through the use of different fitting ranges. Discrepancies between the fit and the data beyond 15 eV are due to a much larger disorder than found in the crystalline As_2O_3 standard [Foster *et al.*¹¹ showed that XANES spectra of a less-ordered As(III) adsorbed to several mineral substrates are smooth beyond 15 eV]. The total amount of residual As in the oxidized $\text{Al}_{0.96}\text{Ga}_{0.04}\text{As}$ film is roughly estimated as $\sim 10\%$ by comparing the magnitude of the As K -absorption-edge step with that of elemental As powder in fluorescence mode after calibrating for the thickness of the As powder along the beam-path.

For the same samples for which near-edge (XANES) analysis is presented above, analysis has also been performed on extended x-ray absorption fine-structure (EXAFS) data, shown in Fig. 2(a), where energies well beyond the E_0 are considered. The raw data are interpolated to an equally spaced grid in photoelectron wave number $k = \sqrt{(2m/\hbar^2)(E - E_0)}$. A least-squares cubic spline function is fit to the smooth background over the k range of 2.8 – 13.7 \AA^{-1} and subtracted from the spectra, isolating the fine-structure oscillations $\chi(k)$. Figure 2(b) shows two scans of the AlGaAs-oxide sample, averaged and weighted by k^3 . Data between the dotted lines (3.9 – 13.5 \AA^{-1}) are Fourier transformed to a pseudoradial distribution function in r space (Å). Major peaks in r space correspond to atomic shells around the excited As atoms (e.g., As–O and As–As) that backscatter the outgoing photoelectron waves. These spectra are then fit to simulations from the multiple scattering code

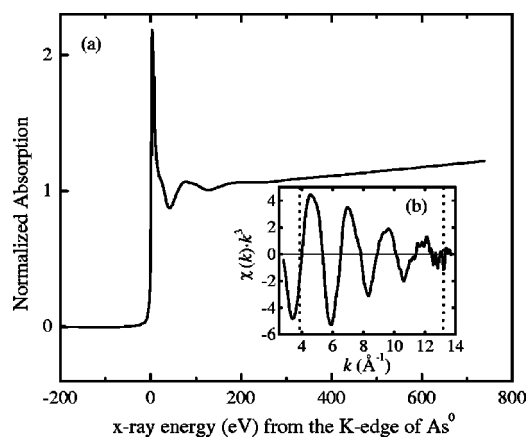


FIG. 2. (a) Normalized raw XAFS data and (b) k^3 -weighted EXAFS oscillation, $\chi(k)k^3$, for the oxidized $\text{Al}_{0.96}\text{Ga}_{0.04}\text{As}$ film.

FEFF6.01 (Ref. 12) and structural parameters (interatomic distances, number of atoms, etc.) are extracted using the program FEFFIT.¹³

In Fig. 3(a), the As K -edge EXAFS r -space spectra of the oxidized $\text{Al}_{0.96}\text{Ga}_{0.04}\text{As}$ sample are shown along with spectra from the standard compounds of elemental As, GaAs, As_2O_3 , and As_2O_5 . Casual inspection indicates that the As atoms in the film are likely to be coordinated with O. The nearest-neighbor distances of elemental As (As–As: 2.52 \AA), and GaAs (As–Ga: 2.45 \AA), as shown in Fig. 3(a), as well as AlAs (As–Al: 2.45 \AA), are far from the peaks of oxidized $\text{Al}_{0.96}\text{Ga}_{0.04}\text{As}$ data. For detailed data fitting (using FEFF6.01 and FEFFIT), a number of structural models are considered, including both interstitial and substitutional As in Al oxides and hydroxides, but none of these models are consistent with the data. However, our XANES analysis above suggests that the residual As is distributed $\sim 80\%$ to As^{3+} and $\sim 20\%$ to As^{5+} sites in the oxide sample. Thus, for an independent EXAFS analysis, theoretical EXAFS spectra are calculated using FEFF6.01 for As_2O_3 and As_2O_5 (Ref. 14) (As_2O_5 has both tetrahedral and octahedral sites) and successfully fit to the measured As_2O_3 and As_2O_5 standard samples with FEFFIT. We have fit the r -space EXAFS data of oxidized $\text{Al}_{0.96}\text{Ga}_{0.04}\text{As}$ to those calculations for the three first shells

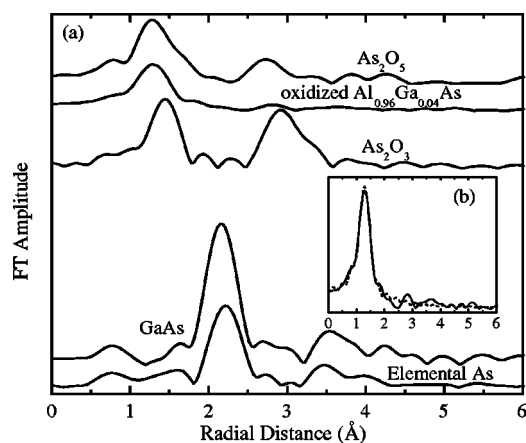


FIG. 3. (a) Magnitudes of the Fourier transform (FT) of the As K -edge data for the oxide film (oxidized $\text{Al}_{0.96}\text{Ga}_{0.04}\text{As}$), elemental As, GaAs, As_2O_3 , and As_2O_5 ; (b) oxide film data (solid line) with the fit of 71% As_2O_3 , 21% As_2O_5 tetrahedral, and 4% As_2O_5 octahedral (dotted line).

(one As₂O₃ site and two As₂O₅ sites). ΔE_0 , the difference between the user-defined theoretical threshold energy and the experimentally determined threshold energy, and S_0 , the many-body amplitude reduction factor, are held at 10 eV and 0.9, respectively (values obtained from fitting the As₂O₃ and As₂O₅ standards). The remaining variable parameters such as compositions of each site (i.e., the multiplying composition factors to S_0), radial distances, and Debye–Waller factors (σ^2 , the rms fluctuation in distances) are floated. The best data fit, shown in Fig. 3(b), is obtained by a combination of 75% As₂O₃, 21% As₂O₅ tetrahedral site, and 4% As₂O₅ octahedral site. Conservatively estimated uncertainties are $\pm 20\%$ of these values. A large Debye–Waller factor ($>0.01 \text{ \AA}^2$) for the As₂O₅ octahedral site results when the two As₂O₅ sites are decoupled, further indicating that the As₂O₅ octahedral site contribution is negligible in the EXAFS data fitting.

Comparing the oxidized Al_{0.96}Ga_{0.04}As data in Fig. 3 with that of the crystalline As₂O₃ and As₂O₅ standards, the essential lack of higher shell scattering features indicates larger disorder and suggests that the residual As in Al_{0.96}Ga_{0.04}As converts to an amorphous matrix of As₂O₃ and As₂O₅ during the wet-oxidation process. Our EXAFS analysis is consistent with the independent XANES analysis of Fig. 1 within uncertainty limits, and both indicate that less than 10% (estimated detection limit) of the As atoms in the oxide film are at any of the considered sites except for As₂O₃ and As₂O₅. This absence of As precipitates in the bulk oxide is consistent with transmission electron microscopy studies,⁷ and with Raman spectroscopy studies⁴ which show that crystalline and amorphous elemental As, clearly present in partially oxidized films, is virtually undetectable in films oxidized to completion (the Al_{0.96}Ga_{0.04}As films in the present work are fully oxidized). While the existence of elemental As at AlGaAs native-oxide/GaAs interfaces has been supported by electrical measurements,^{4,15} any As-rich interfacial region in the present work has either been removed with the GaAs substrate, or is below our detection limit.

In previous Raman spectroscopy studies by Ashby and co-workers,^{4,5} amorphous arsenic oxide in oxidized Al_{0.98}Ga_{0.02}As films has a broad, weak spectral signature and is identified only as As₂O₃ (based on an earlier study which did not include As₂O₅). The wet-thermal oxidation reaction⁵ producing As₂O₃ is



Thermochemical calculations¹⁶ at 400 °C (673 K) for the reaction



indicate that the formation of As₂O₅ is also thermodynamically favorable ($\Delta G^{673} = -157 \text{ kJ/mol}$), though less so than for As₂O₃ [Eq. (1), $\Delta G^{673} = -479 \text{ kJ/mol}$]. The phase of As₂O₅ in Eq. (2) is uncertain as, under equilibrium conditions, bulk As₂O₅ is known to decompose to As₂O₃ at 315 °C.¹⁷ The balance between rates of formation and reduc-

tion of arsenic oxide at the oxidation reaction front is believed to play a role in regulating AlAs oxidation rates.⁶ Like As₂O₃,⁵ the reduction of As₂O₅ to As by H₂ is thermodynamically favored ($\Delta G^{673} = -451 \text{ kJ/mol}$). In addition, the formation of arsine, a second volatile species which could remove As from the oxide, is also favorable from reaction of As₂O₅ and H₂ ($\Delta G^{673} = -298 \text{ kJ/mol}$).

In summary, both EXAFS and XANES analysis show that the residual As in wet-oxidized AlGaAs films is distributed between a mixture of $\sim 80\%$ As³⁺ and $\sim 20\%$ As⁵⁺ sites that are locally similar to As₂O₃ and As₂O₅. To be consistent with our data, less than about 10% of the As atoms can be in elemental As, GaAs, or in interstitial or substitutional sites in Al oxides or Al hydroxides.

This work was supported in part by Air Force Office of Scientific Research Grant No. F49620-98-1-0120. The MRCAT is supported by the U.S. Department of Energy (DOE) under Contract No. DE-FG02-94-ER45525 and the member institutions. Use of the APS was supported by the U.S. DOE, under Contract No. W-31-102-Eng-38.

¹J. M. Dallesasse, N. Holonyak, Jr., A. R. Sugg, T. A. Richard, and N. El-Zein, *Appl. Phys. Lett.* **57**, 2844 (1990).

²See, K. D. Choquette, K. M. Geib, C. I. H. Ashby, R. D. Twesten, O. Blum, H. Q. Hou, D. M. Follstaedt, B. E. Hammons, D. Mathes, and R. Hull, *IEEE J. Sel. Top. Quantum Electron.* **3**, 916 (1997).

³See, C. B. DeMelo, D. C. Hall, G. L. Snider, D. Xu, G. Kramer, and N. El-Zein, *Electron. Lett.* **36**, 84 (2000), and references therein.

⁴C. I. H. Ashby, J. P. Sullivan, P. P. Newcomer, N. A. Missert, H. Q. Hou, B. E. Hammons, M. J. Hafich, and A. G. Baca, *Appl. Phys. Lett.* **70**, 2443 (1997).

⁵C. I. H. Ashby, J. P. Sullivan, K. D. Choquette, K. M. Geib, and H. Q. Hou, *J. Appl. Phys.* **82**, 3134 (1997).

⁶C. I. H. Ashby, M. M. Bridges, A. A. Allerman, B. E. Hammons, and H. Q. Hou, *Appl. Phys. Lett.* **75**, 73 (1999).

⁷R. D. Twesten, D. M. Follstaedt, and K. D. Choquette, *Proc. SPIE* **3003**, 55 (1997).

⁸*X-Ray Absorption: Principles, Applications, Techniques of EXAFS, SEXAFS and XANES*, edited by D. C. Koningsberger and R. Prins (Wiley, New York, 1988).

⁹P. J. Durham, in *X-Ray Absorption: Principles, Applications, Techniques of EXAFS, SEXAFS and XANES*, edited by D. C. Koningsberger and R. Prins (Wiley, New York, 1988), Chap. 2, pp. 53–84; A. Bianconi, *ibid.*, Chap. 11, pp. 573–662.

¹⁰C. U. Segre, N. E. Leyarovska, L. D. Chapman, W. M. Lavender, P. W. Plag, A. S. King, A. J. Kropf, B. A. Bunker, K. M. Kemner, P. Dutta, R. S. Duran, and J. Kaduk, in *CP521, Synchrotron Radiation Instrumentation: Eleventh U.S. National Conference*, edited by P. Pianetta, J. Arthur, and S. Brennan (American Institute of Physics, New York, 2000), pp. 419–422.

¹¹A. L. Foster, G. E. Brown, Jr., and G. A. Parks, *Environ. Sci. Technol.* **32**, 1444 (1998).

¹²J. J. Rehr, R. C. Albers, and S. I. Zabinsky, *Phys. Rev. Lett.* **69**, 3397 (1992).

¹³E. A. Stern, M. Newville, B. Ravel, Y. Yacoby, and D. Haskel, *Physica B* **208&209**, 117 (1995).

¹⁴M. C. G. Passeggi, Jr., I. Vaquila, and S. J. Sferco, *Phys. Rev. B* **50**, 2090 (1994).

¹⁵P. A. Parikh, Ph.D. thesis, University of California, Santa Barbara (1997).

¹⁶O. Kubaschewski, C. B. Alcock, and P. J. Spencer, *Materials Thermochemistry* (Pergamon, London, UK, 1993).

¹⁷C. W. Wilmsen, *Thin Solid Films* **39**, 105 (1976).